

# REPORT DOCUMENTATION PAGE

AFRL-SR-AR-TR-04-

Public reporting burden for this collection of information is estimated to average 1 hour per response, including the time for reviewing instructions, data needed, and completing and reviewing this collection of information. Send comments regarding this burden estimate or, any other aspect of this burden to Department of Defense, Washington Headquarters Services, Directorate for Information Operations and Reports (0704-01-4302). Respondents should be aware that notwithstanding any other provision of law, no person shall be subject to any penalty for failing to comply with a valid OMB control number. PLEASE DO NOT RETURN YOUR FORM TO THE ABOVE ADDRESS.

0069

1. REPORT DATE (DD-MM-YYYY)		2. REPORT TYPE Final Progress Report		3. DATES COVERED (From - To) April 2002-2003	
4. TITLE AND SUBTITLE Direct Write Laser Lithography System		5a. CONTRACT NUMBER F49620-02-1-0347			
		5b. GRANT NUMBER			
		5c. PROGRAM ELEMENT NUMBER			
6. AUTHOR(S) Axel Scherer		5d. PROJECT NUMBER			
		5e. TASK NUMBER			
		5f. WORK UNIT NUMBER			
7. PERFORMING ORGANIZATION NAME(S) AND ADDRESS(ES) Axel Scherer MC 200-36, (626) 395-4691 Caltech, Pasadena CA 91125					
8. SPONSORING / MONITORING AGENCY NAME(S) AND ADDRESS(ES) Dr. Gernot S. Pomrenke AFOSR Program Manager Optoelectronics and nano-technology			9. SPONSOR/MONITOR'S ACRONYM(S) Ballston Common Towers III 4015 Wilson Blvd, Room 713 Arlington VA 22203-1954		
			10. SPONSOR/MONITOR'S REPORT NUMBER(S)		
12. DISTRIBUTION / AVAILABILITY STATEMENT <i>Distribution Statement A: Approved for public release, distribution unlimited</i>					
13. SUPPLEMENTARY NOTES					
14. ABSTRACT <p>The Heidelberg Instruments laser writer was purchased in July 2002, arrived in November 2002, and was fully operational after several months of optimization and hardware troubleshooting in April 2003. At present, this instrument is used for optical beam-writing of UV lithography masks, and will be employed in tandem with a recently purchased MA6/BA6 mask aligner for rapid prototyping in nanobiotechnology and nanophotonics research at Caltech. It is presently also used for direct-writing of microfluidic replication molding dies, and has enabled the demonstration of the first integrated elastomeric one-way microfluidic valve. It has been successfully applied towards the microfabrication of electrostatic contacts onto optical devices that are back-filled with liquid crystals and electro-optic polymers with the goal of constructing electrically tuneable optical devices.</p>					
15. SUBJECT TERMS					
16. SECURITY CLASSIFICATION OF: a. REPORT		17. LIMITATION OF ABSTRACT b. ABSTRACT	18. NUMBER OF PAGES c. THIS PAGE	19a. NAME OF RESPONSIBLE PERSON 19b. TELEPHONE NUMBER (include area code)	

# DISTRIBUTION STATEMENT

Approved for Public Release

Distribution Unlimited

Final Report, Award F49620-02-1-0347

AFOSR/DURIP

P.I. Axel Scherer, Caltech

## Progress report: DURIP award "Direct Write Laser Lithography System"

### Abstract

The Heidelberg Instruments laser writer was purchased in July 2002, arrived in November 2002, and was fully operational after several months of optimization and hardware troubleshooting in April 2003. At present, this instrument is used for beam-writing optical lithography masks, and will be employed in tandem with a recently purchased MA6/BA6 mask aligner for rapid prototyping in nanobiotechnology and nanophotonics research at Caltech. It is presently also used for direct-writing of microfluidic replication molding dies, and has enabled the demonstration of the first integrated elastomeric one-way microfluidic valve. It has also been applied towards the microfabrication of electrostatic contacts onto optical devices (Figure 1&2) that are back-filled with liquid crystals and electro-optic polymers with the goal of constructing electrically tuneable optical devices. The first devices of this sort were fabricated during the summer of 2003 (Figure 2), and will be described below.

Electrically tuned ring resonators (Figure 1&2) and photonic crystal lasers (Figure 5) were demonstrated by using this system. These device work by surrounding or infiltrating photonic crystal laser cavities with nematic liquid crystal. Our laser represents the first of a new class of adaptive devices incorporating optics, fluidics, and electronics. A liquid crystal cell is constructed by surrounding the photonic crystal or ring resonator between contacts, which serve as the modulating electrodes. Applying a voltage across the cell realigns the liquid crystal, modifies the cavity's optical path length, and shifts the resonator wavelength. Applying 20 volts across the cell blue-shifts the lasing wavelength by 1.2 nanometers. The tuning exhibits a threshold coincident with that of the liquid crystal realignment, is independent of field polarity and features a slight hysteresis.

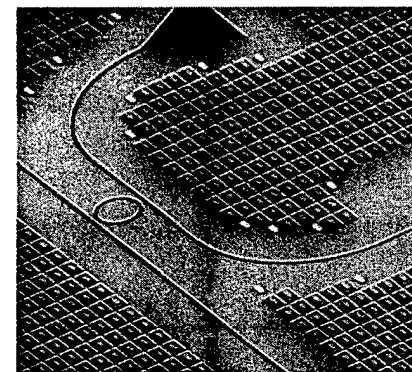


Figure 1: SEM micrograph of a ring resonator such as the one used for the liquid crystal tuning demonstration

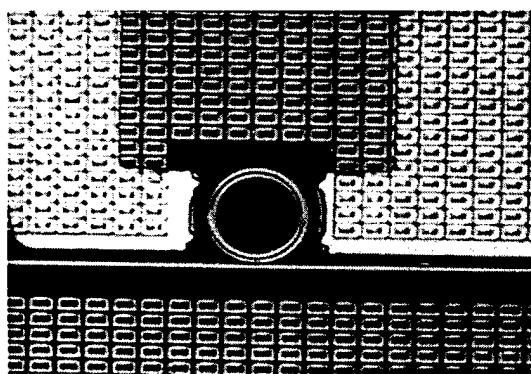


Figure 2: Electrostatic gold contacts aligned to a ring resonator with the help of the Heidelberg Instruments writer

### Technical Details

The devices developed by using our laser writer combine nonlinear optical materials, electronics, and fluidics, all integrated within devices to provide increased functionality and utility. Microfabricated photonic crystals (PCs) enable the microscopic manipulation of light within two- and three-dimensionally (2D and 3D) periodic geometries (1,2), and have been used to realize efficient nano-scale optical cavities and lasers (3). Light emitted from a PC laser, although generated from a semiconductor slab, can be concentrated in the air pores that define the PC. We have recently used this effect to develop PC laser

Final Report for F49620-02-1-0347

A. Scherer, Caltech

sensors in which the maximum optical field occurs within a hole etched through the center of the laser cavity (4). Such lasers provide efficient interaction between light and liquid analytes and have so far been used for the precise determination of the index of refraction of ultra-small volumes of back-filled liquids by observing shifts in the laser spectrum. Until now, it has been difficult to actively tune the emission frequency of PC lasers by deliberately changing the refractive index of the material inside of the cavity. To electrostatically tune PCs, infiltration of liquid crystals (LCs) into the pores of such structures was proposed several years ago (5). Here we report the first successful LC tuned 2D PC lasers – devices in which the lasing frequency can be electrostatically controlled with an applied gate voltage.

The resonant wavelength of an optical cavity can be tuned by adjusting the cavity's refractive index (Figure 4), and hence its optical path length. Such tuning has previously been accomplished in a 2D PC laser by lithographically controlling the local cavity geometry (7) or by filling of the holes of the PC with liquids of different refractive index (4). Several groups have also demonstrated dynamic thermal tuning of PCs with infiltrated LCs (8-10) and more recently electrical tuning via the controlled orientation of LCs has been reported (11-13). Electrically

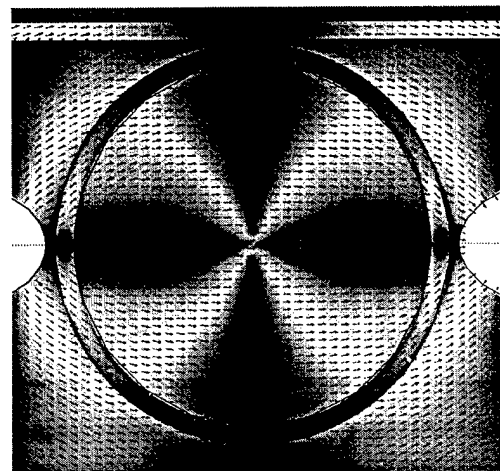


Figure 3: Distribution of the electrostatic field between two lithographically aligned contacts aligned to a ring resonator

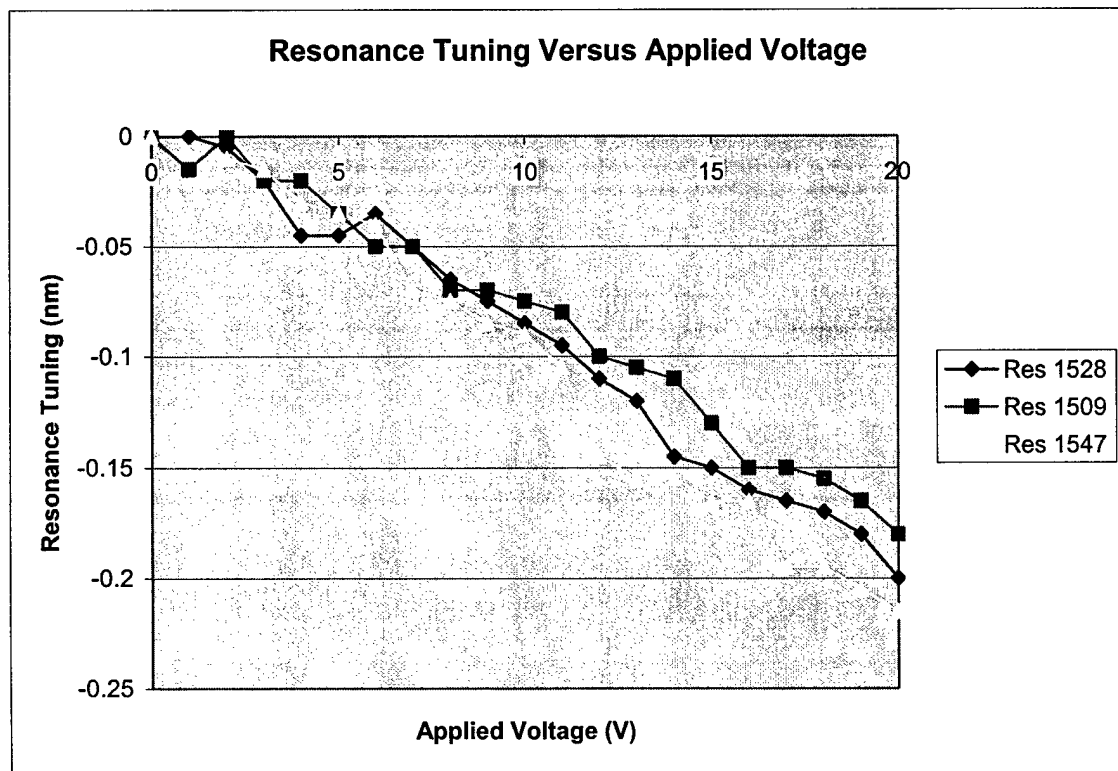


Figure 4: Electrostatic tuning induced shifts in the resonance frequency of a ring resonator. The three curves are measured from three different resonators and show a linear tuning behavior with applied voltage.

tuned PC lasers presented in this work are the smallest tunable lasers to date, and our work leads to the understanding of nonlinear behavior in high-Q nanocavities. We report on electrically tuning of PC lasers by controlled alignment of infiltrated nematic LC.

Liquid crystals offer a relatively large birefringence and corresponding large refractive index tuning ranges. Before LC tunable PC lasers can be constructed, several design constraints need to be addressed. When the PC is infiltrated with a liquid, the refractive index contrast decreases. This results from the ambient refractive index change from that of air ( $n=1$ ) to that of a LC ( $n \sim 1.45-1.7$ ). The lower resulting refractive index contrast in turn narrows the photonic bandgap, decreasing the confinement of the light and reducing the cavity's quality factor ( $Q$ ). Thus, the relatively high refractive indices of LCs demand a significant re-design of the laser cavity geometry. Moreover, their large birefringence can scatter light if the LC is not aligned uniformly. Therefore, the nematic LC chosen for this study (MLC-6815 from Merck) has a deliberately low refractive index ( $n_e = 1.519$ ,  $n_o = 1.467$  at 589nm) and a modest birefringence (0.05 at 589nm). The  $Q$  of the PC cavity can then be sufficiently optimized to enable lasing even after infiltration of the PC. Of course, this choice also results in a reduced tuning range of the PC lasers.

To accommodate the low refractive index contrast, a new high  $Q$  PC cavity design was used (14). A SEM image of the PC laser cavity is shown in Fig. 1. The device geometry optimized the  $Q$  of one of the dipole modes supported by the laser cavity to above 3000, even when operated within an ambient refractive index of  $n \sim 1.5$ . PC lasers using this design were defined within InGaAsP quantum well material and fabricated using a combination of electron beam lithography and dry etching. The details of the laser fabrication procedure have been previously described (15). To construct the LC cell around the lasers, we first attached the laser sample along with two spacers to an indium tin oxide (ITO) transparent conducting plate with polymethylmethacrylate (PMMA). Next, a drop of the LC was placed on the PC sample and then the 0.3 mm thick top ITO plate was glued to the spacers. The spacers were sufficiently thick to obtain an estimated 15  $\mu\text{m}$  gap between the sample and top ITO electrode, which was chosen to minimize absorption at 1.55  $\mu\text{m}$ , exhibiting 92% transmission at that wavelength. The LC was then heated above the clearing point (67°C) on a hotplate at 90°C for 5 minutes to help ensure complete infiltration into the PC. Finally electrical leads were attached to the ITO plates with conductive tape to complete the LC cell. A cross section of the fully assembled LC cell appears in Fig. 2 A.

Samples were measured using a micro-photoluminescence setup (15). Lasing after LC infiltration was confirmed by the recording of a characteristic output power versus input power curve (L-L curve). The PC lasers were pumped with 5.3 mW from a semiconductor laser diode at 830 nm with a pulse length of 15 ns and a periodicity of 1.5  $\mu\text{s}$ . Pump light was transmitted through the top plate and the LC onto the PC slab. Much of the light was also transmitted through the slab, as it did not get absorbed in the semiconductor quantum wells. During the optical pumping of the PC cavities, the refractive index of the LC was changed by application of an electrostatic field between the top ITO electrode and the InP wafer substrate. The expected tuning range strongly depends on the LC's refractive indices and the birefringence at the lasing wavelength  $\lambda \sim 1.55 \mu\text{m}$ , the spontaneous (zero-field) LC orientation, and the electric field pattern generated by the electrodes. To the best of our knowledge, the optical properties of MLC-6815 have not been characterized at 1.55  $\mu\text{m}$  and were estimated by back-filling the laser cavities

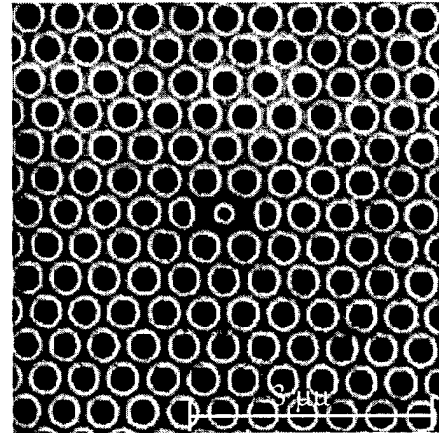


Fig. 5. Scanning electron micrograph of fabricated 2D PC laser. Periodicity of holes is 500 nm, radii of holes are  $\sim 165$  nm, radius of defect hole is  $\sim 100$  nm.

with index matched fluids. By comparing the lasing wavelength shift in air to that of the index matched fluids and LC, we determined the average refractive index of the LC at  $1.55 \mu\text{m}$  to be close to its known value at 589 nm. Accordingly, we used the specified values at 589 nm for  $n_e$  and  $n_o$  in the following analysis. Polarization interference microscopy was also used to also determine the bulk birefringence of the LC and to reveal information of any spontaneous alignment of the top cladding layer (16). The observed interference patterns indicated significant homogenous LC alignment, parallel to the plane of the PC in the bulk part of the top cladding layer. However, due to surface effects this did not guarantee homogenous alignment in the proximity of the PC membrane (17).

To establish a baseline for the laser tuning range, the LC is assumed to initially be randomly orientated, and the influence of the applied voltage used for alignment of the LC is modeled using electrostatic simulations of the generated electric field patterns (Fig. 2 B and C). These simulations indicate that the LC in the top cladding can be aligned vertically, but the electric field is sharply damped in the holes of the PC due to screening by the conducting PC membrane. The lasing mode under investigation not only samples the refractive index in the holes of the PC, but also has an evanescent field in the top cladding layer and therefore is influenced by the refractive index in that region. Therefore, tuning of the cavity can be achieved by changing the refractive index in the holes or in the cladding layers. For the TE-like lasing modes, the contribution of a LC molecule towards the hole or cladding refractive indices is given by (18):

$$1/n^2 = \cos^2(\theta)/n_e^2 + \sin^2(\theta)/n_o^2 \quad (1)$$

where  $n$  is the refractive index of interest ( $n_{\text{top}}$ ,  $n_{\text{bottom}}$ ,  $n_{\text{hole}}$ ) and  $\theta$  is the angle between the nematic LC director and the PC lasing mode's polarization vector. We infer from Eq. (1) that as a LC molecule is rotated relative to the PC plane, the effective refractive index experienced by the lasing mode ranges from  $n_e$  to  $n_o$ . The average refractive index due to a randomly oriented LC is given by:

$$n_{\text{avg}} = \sqrt{(n_e^2 + 2n_o^2) / 3} \quad (2)$$

Thus, the effective refractive index of randomly oriented LC in this study is approximately 1.483, Eq.(2).

The LC's threshold and saturation voltages were used to help understand the dynamic tuning of the PC laser. Polarization interference microscopy was used to determine the threshold voltage and the onset of LC realignment. The applied voltage was slowly ramped until the observed interference pattern changed, indicating a change in the LC orientation. By using this method, we have measured threshold and saturation voltages of approximately 4 V and 8 V, which agree well with the LC specifications. This indicates that most of the voltage drop in the cell is across the top LC cladding. The

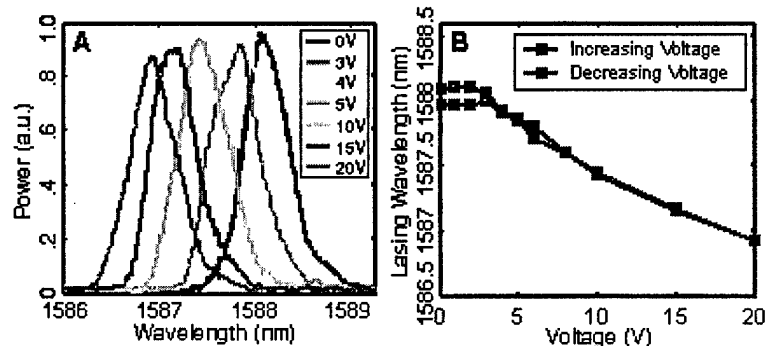


Fig. 3. Demonstration of laser tuning via LC realignment. A) Laser spectra taken with an applied voltage ranging from 0-20 V across the LC cell. The threshold for tuning is 4 V, coinciding with the measured threshold voltage for the LC. A maximum blue-shift of 1.2 nm was measured with an applied 20 V. B) Lasing wavelength versus applied voltage for a voltage ramp cycle. Although the tuning rate lessens at higher voltage, the data suggest saturation was not even reached at 20 V and further tuning may be possible with stronger fields. The tuning is reversible but demonstrates a slight hysteresis at low fields which may be due to residual LC alignment.

resistance of the cell was measured to be in excess of  $10^8$  Ohms and thermal heating and tuning of the laser due to leakage currents were negligible.

We demonstrate LC tuning of the PC laser by recording the lasing wavelength as a function of the voltage applied across the LC. Our electrostatic simulation results predict that the LC in the top cladding should align vertically to the surface, lowering  $n_{top}$  from 1.483 to 1.467 and blue-shifting the lasing wavelength. When the voltage is varied from 0 to 20 V, we observe a corresponding blue-shift in Fig. 3 A. The wavelength shift starts at 4 V, the threshold voltage of the LC, signaling the existence of a Freedericksz transition. A maximum tuning of 1.2 nm is observed at 20 V and the tuning appears to be independent of the field polarity, but shows a slight hysteresis that can be a result of residual LC alignment (Fig. 3 B). The tuning behavior at strong fields suggests surface anchoring heavily influences the alignment dynamics of the LC in the vicinity of the PC membrane. The protracted transition to a saturated aligned state further indicates the LC spontaneously aligns homogenously to the PC membrane. As the electric field is steadily increased, LC molecules closer to the membrane surpass the free energy barrier and align with the field (Fig. 4 A, B, and C).

### Impact

The Heidelberg Instruments laser writer has been successfully installed and has enabled the demonstration of electrical tuning of optical cavities by controlling the orientation of an infiltrated LC, and we achieved a tuning of 1.2 nm upon application of 20 V across a LC cell and this tuning displayed threshold behavior coincident with that of the LC. The tuning range may be broadened further by optimizing the cavity geometry, infiltrating the cavity with LCs featuring larger birefringence, increasing the effectiveness of LC alignment with in-plane electrodes or alignment layers, and by controlling the alignment in the holes of the PC. Such enhancements can potentially increase the tuning range of a PC laser beyond 20 nm. Furthermore, a LC infiltrated PC laser provides an excellent and unique opportunity to probe the behavior of LCs confined in nanoscale geometries and enables the simultaneous study of the LC's nonlinear optical interaction with an intense optical field.

### References and Notes

1. E. Yablonovitch, *Phys. Rev. Lett.*, **58**, 2059 (1987).
2. S. John, *Phys. Rev. Lett.*, **58**, 2486 (1987).
3. O. Painter, et al., *Science*, **284**, 1819 (1999).
4. M. Loncar, A. Scherer, and Y. Qiu, *Appl. Phys. Lett.* **82**, 4648, (2003).
5. K. Busch and S. John, *Phys. Rev. Lett.* **83**, 967 (1999).
6. B. Maune, et al. in press.
7. O. Painter, et al. *IEEE Photonics Technol. Lett.* **12**, 1126 (2000).
8. S. W. Leonard et al., *Phys. Rev. B* **61**, R2389, (2000).
9. G. Mertens, T. Roder, R. Schweins, K. Huber, and H. S. Kitzerow, *Appl. Phys. Lett.* **80**, 1885, (2002).
10. C. Schuller, F. Klopff, J. P. Reithmaier, M. Kamp, and A. Forchel, *Appl. Phys. Lett.* **82**, 2767, (2003).
11. D. Kang, J. E. MacLennan, N. A. Clark, A. A. Zakhidov, and R. H. Baughman, *Phys. Rev. Lett.* **86**, 4052 (2001).
12. Y. Shimoda, M. Ozaki, and K. Yoshino, *Appl. Phys. Lett.* **79**, 3627, (2001).
13. R. Ozaki, T. Matsui, M. Ozaki, and K. Yoshino, *Appl. Phys. Lett.* **82**, 3593, (2003).
14. M. Loncar, et al. in preparation.
15. M. Loncar, T. Yoshie, A. Scherer, P. Gogna, and Y. Qiu, *Appl. Phys. Lett.* **81**, 2680, (2002).
16. S. Kumar, *Liquid Crystals* (Cambridge Univ. Press, Cambridge, UK, 2001).
17. A. A. Sonin, *The Surface Physics of Liquid Crystals* (Gordon and Breach Publishers, Amsterdam, Netherlands, 1995).
18. B. E. A. Saleh, and M. C. Teich, *Fundamentals of Photonics* (Wiley, New York, ed. 1, 1991).
19. L. Blinov, in *Handbook of Liquid Crystals*, D. Demus, J. Goodby, G. W. Gray, H. W. Spiess, V. Vill, Eds. (Wiley-VCH, New York, 1998) vol. 1, chap. 9.
20. G. P. Crawford, M. Vilfan, J. W. Doane, and I. Vilfan, *Phys. Rev. A* **43**, 835, (1991).
21. G. P. Crawford, D. W. Allender, J. W. Doane, M. Vilfan, and I. Vilfan, *Phys. Rev. A* **44**, 2570, (1991).
22. The principle investigator would like to thank Brett Maune, Mark Adams, and David Barsic, for their work on installing and optimizing the laser writer. Funding for some of this work was also provided by Jag Shah from DARPA under the CS-WDM program (Contract No. N00421-02-D-3223) is also gratefully acknowledged.